Albedo of Coastal Landfast Sea Ice in Prydz Bay, Antarctica: Observations and Parameterization

Qinghua YANG[*1,2], Jiping LIU[3], Matti LEPPÄRANTA[4], Qizhen SUN[1], Rongbin LI[1], Lin ZHANG[1], Thomas JUNG[2,5], Ruibo LEI[6], Zhanhai ZHANG[6], Ming LI[1], Jiechen ZHAO[1], and Jingjing CHENG[7]

[1]*Key Laboratory of Research on Marine Hazards Forecasting, National Marine Environmental Forecasting Center, Beijing* 100081

[2]*Alfred Wegener Institute, Helmholtz Centre for Polar and Marine Research, Bremerhaven* 27570, *Germany*

[3]*State Key Laboratory of Numerical Modeling for Atmospheric Sciences and Geophysical Fluid Dynamics, Institute of Atmospheric Physics, Chinese Academy of Sciences, Beijing* 100029

[4]*University of Helsinki, Helsinki* 00014, *Finland*

[5]*University of Bremen, Bremen* 28334, *Germany*

[6]*Key Laboratory for Polar Science of the State Oceanic Administration, Polar Research Institute of China, Shanghai* 200136

[7]*National Center of Ocean Standards and Metrology, Tianjin* 300112

ABSTRACT

The snow/sea-ice albedo was measured over coastal landfast sea ice in Prydz Bay, East Antarctica (off Zhongshan Station) during the austral spring and summer of 2010 and 2011. The variation of the observed albedo was a combination of a gradual seasonal transition from spring to summer and abrupt changes resulting from synoptic events, including snowfall, blowing snow, and overcast skies. The measured albedo ranged from 0.94 over thick fresh snow to 0.36 over melting sea ice. It was found that snow thickness was the most important factor influencing the albedo variation, while synoptic events and overcast skies could increase the albedo by about 0.18 and 0.06, respectively. The *in-situ* measured albedo and related physical parameters (e.g., snow thickness, ice thickness, surface temperature, and air temperature) were then used to evaluate four different snow/ice albedo parameterizations used in a variety of climate models. The parameterized albedos showed substantial discrepancies compared to the observed albedo, particularly during the summer melt period, even though more complex parameterizations yielded more realistic variations than simple ones. A modified parameterization was developed, which further considered synoptic events, cloud cover, and the local landfast sea-ice surface characteristics. The resulting parameterized albedo showed very good agreement with the observed albedo.

Key words: Antarctic, sea ice, albedo, observation, parameterization

---

1. Introduction

Satellite passive-microwave observations show that the total area of Antarctic sea ice in winter has been increasing by $17\,100 \pm 2300$ km^2 yr^{-1} since the late 1970s (e.g., Liu and Curry, 2010; Parkinson and Cavalieri, 2012). To understand and model the variability of Antarctic sea ice cover, accurate knowledge and parameterization of the albedo are needed. To date, most *in-situ* studies of solar radiation in polar seas have been carried out in the Arctic (e.g., Perovich et al., 2002; Perovich and Polashenski, 2012), while very limited observations of radiative characteristics and optical properties (especially albedo) have been performed over Antarctic sea ice

(e.g., Allison et al., 1993; Brandt et al., 2005; Vihma et al., 2009; Weiss et al., 2012). Moreover, all the existing observational records over Antarctic sea ice are too short and do not cover the seasonal evolution and interannual variability, and sea-ice conditions around Antarctica differ significantly from those in the Arctic (Wendler et al., 2000).

The albedo of snow and sea ice is a complex function of surface layer characteristics and illumination conditions, which depend on the atmospheric cloudiness and humidity and the solar zenith angle. Snow and sea ice have high reflectance in the visible band but they are moderately absorptive in the near infrared (Curry et al., 2001). The snow albedo depends on the grain size and shape, snow thickness and optical properties of its underlying surface (Grenfell and Perovich, 1984; Leppäranta et al., 2013). The sea-ice albedo is also affected by ice types (e.g., new ice, first-year ice, mul-

* Corresponding author: Qinghua YANG

  Email: yqh@nmefc.gov.cn

tiyear ice, ridged ice, brash ice), ice thickness, brine pockets and gas bubbles in the ice, surface roughness, and melt ponds (Perovich et al., 2002). Due to surface-layer evolution, the snow/ice albedo shows obvious seasonal variation, i.e., the albedo is highest in the dry snow period and significantly reduced in the melting period (Perovich et al., 2002; Perovich and Polashenski, 2012). Weather events, such as snowfall and blowing snow, can affect the albedo by changing the surface properties (Brandt et al., 2005). Cloud cover can change the directional distribution of incident solar radiation and therefore increase the snow/ice surface albedo (Curry et al., 2001). The albedo may also change with solar zenith angle (Pirazzini, 2004).

Currently, global climate models use a number of snow/sea-ice albedo parameterizations with different complexities (e.g., Barry, 1996; Curry et al., 2001; Liu et al., 2007). However, sea-ice albedo parameterizations have been largely determined and validated with observations that have been collected in the Arctic (e.g., Curry et al., 2001; Liu et al., 2007), and little is known about how well these parameterizations perform for Antarctic sea ice (Weiss et al., 2012), especially the complex parameterizations that consider snow thickness and ice thickness. Thus, continuous time series of the Antarctic sea ice albedo are required to quantify the influence of different factors on variations in albedo, and provide a dataset for evaluating and developing Antarctic sea-ice albedo parameterizations.

Antarctic landfast sea ice is an important connection between the ice sheet and pack ice/ocean (Fraser et al., 2012) and has gained much attention in recent years. Because of its immobility, repeated measurements of near-coastal landfast

sea ice are a feasible way to examine the temporal evolution of Antarctic sea ice (e.g., Smith et al., 2001; Lei et al., 2010; Heil et al., 2011; Hoppmann et al., 2015). The coastal landfast sea ice in Prydz Bay, East Antarctica, is normally first-year sea ice, crushed and melted completely in January or February and refrozen by the end of February or early March; so, the ice-free period is generally less than 1 month in duration (Lei et al., 2010). To improve our understanding of albedo variation over Antarctic sea ice, we carried out radiation measurements on the landfast sea ice at a fixed site near Zhongshan Station in Prydz Bay. This site has been operational every year in austral spring and early summer since 2010.

In this paper, *in-situ* measurements of surface albedo near Zhongshan Station in 2010 and 2011 are analyzed. We describe the variations in albedo over Antarctic coastal landfast sea ice during austral spring and early summer. We then investigate the primary factors influencing the variations in observed albedo, particularly the effects of synoptic events, including snowfall, blowing snow and overcast skies. Finally, we evaluate the commonly used albedo parameterizations with different levels of complexity to determine to what extent they can produce the observed albedo.

2. Observation site and measurement description

The site of the sea-ice radiation measurements is located in the coastal area off Zhongshan Station [(69°22′S, 76°22′E); Fig. 1]. Meanwhile, the meteorological data were
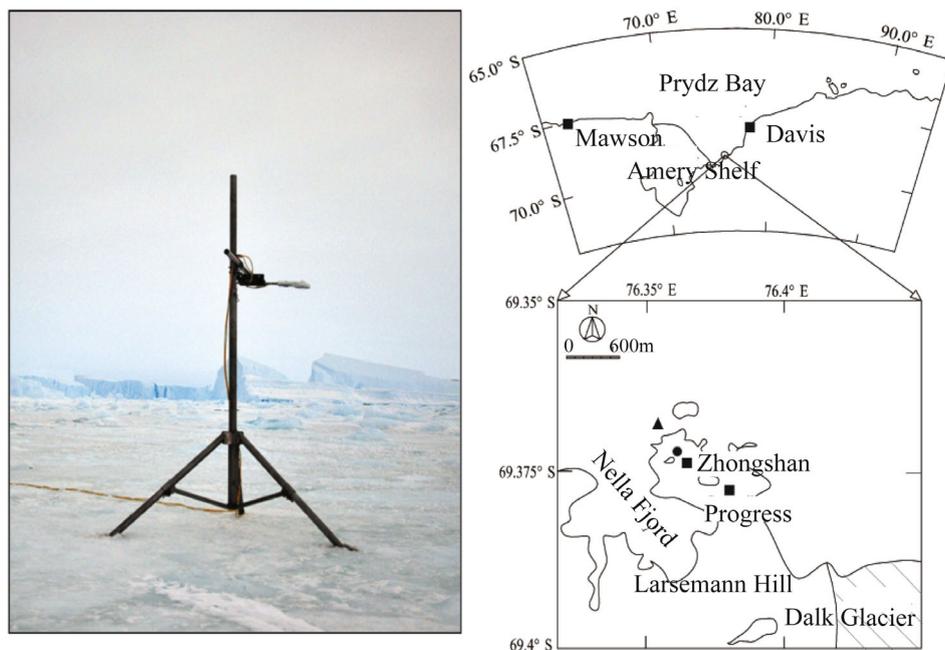
Fig. 1. Location of landfast sea ice surface measurements near Zhongshan Station in 2010 and 2011. The solid triangle denotes the observation site, the solid circle marks Zhongshan Station, and the solid squares refer the locations of Zhongshan, Mawson, Davis and Progress II stations.

collected at a manned weather station, which is 1 km in-land from the sea ice observation site at 15 m above the sea level. Solid precipitation is measured every 12 hours at the Russian Progress II station (located ~1 km from the sea ice observation site). The meteorological conditions during the period of sea-ice observations in 2010 and 2011 are shown in Fig. 2. In 2010, the surface air temperature was below 0°C before 9 December; whereas, in 2011, most of the daily maximum air temperatures exceeded 0°C after 11 November (Fig. 2a). As a result, surface melting in 2011 started around 20 days earlier than that in 2010. The relative humidity was generally low (mostly below 60%; Fig. 2b), which is typical for the coast of the Antarctic continent. The mean snowfall amount was lower in 2011 than in 2010, i.e., the total solid precipitation in August, September, October and November of 2010/2011 was 46.9/14.7, 15.9/17.2, 7.7/5.2, and 12.5/0.4 mm SWE (snow water equivalent), respectively (Fig. 2c). The mean cloudiness for August, September, Octo-ber and November in the two years ranged from 48% to 85%, but there were more clear-sky days and fewer cloudy days in 2011 than in 2010 (Fig. 2d). The mean wind speed (Fig. 2e) ranged from 4.8 m s^{-1} to 8.3 m s^{-1}, and the surface wind di-rection was primarily northeast (approximately 77.1% of the observation time).

Four broadband components of radiation, including downward and upward shortwave (Sw_{in}/Sw_{out}) and long-wave (Lw_{in}/Lw_{out}) fluxes, were measured over the landfast sea ice from 27 July to 15 December 2010 and from 1 August to 30 November 2011.

The shortwave and longwave radiation were measured with a net radiometer mounted at 1.5 m above the surface on a 3-m high tripod (Fig. 1, left panel). The net radiome-ter includes a pyranometer and a pyrgeometer. The pyra-nometer measures incoming and outgoing shortwave radia-tion, and the pyrgeometer measures downward and upward longwave radiation. The spectral bands of the pyranometer
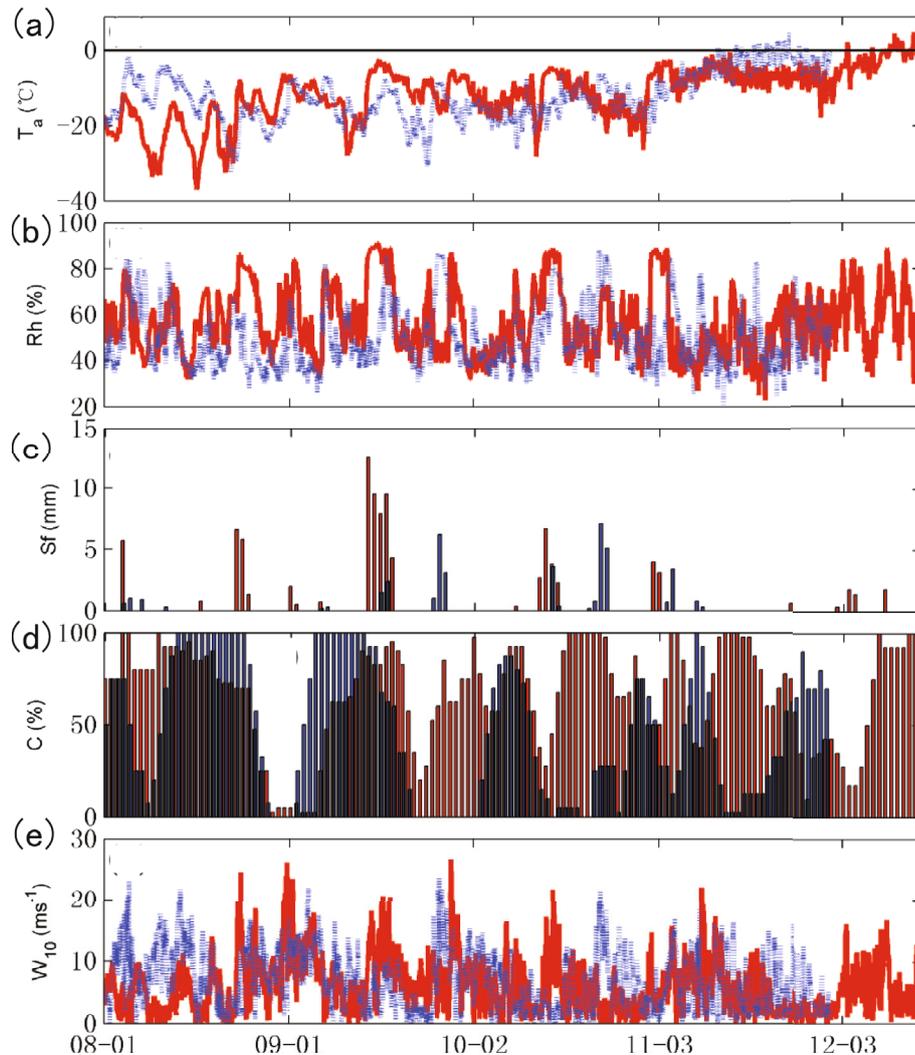
Fig. 2. Time series of (a) hourly surface air temperature, (b) hourly surface relative humidity, (c) daily solid precipitation (in water equivalent depth), (d) daily observed mean cloudiness and (e) hourly surface wind speed. The red coloring denotes 2010 (1 August to 15 December) and the blue coloring denotes 2011 (1 August to 30 November).

are 310–2800 nm, and the spectral bands of the pyrgeometer are 4500–42 000 nm.

The fluxes were recorded every minute. The domes of the radiation sensors were checked between 1230 and 1300 LST (local time) every day, and ice, snow and/or frost flower cover was seldom observed during the campaign. Because surface melt might cause some tilting of the instrument, the horizontal levelling of the radiometers was also checked and adjusted if necessary. The uncertainty associated with the radiation measurements is ±5%. We calculated snow/bare-ice surface temperature from the downward/upward longwave fluxes with a fixed emissivity following the method of Pirazzini et al. (2006). Because albedo measurements are not reliable under large solar zenith angles (Vihma et al., 2009), the albedo was calculated from the ratio Sw_{in}/Sw_{out} for zenith angles lower than 80°, which is consistent with Pirazzini (2004) and Järvinen and Leppäranta (2013).

Snow thickness was measured almost every day using a ruler with an accuracy of ±0.2 cm. A rough estimation of the snow grain size at the surface was made visually using a scaled magnifier. To avoid disturbances to the albedo measurements, the snow observations were made near the view of the downward-facing pyranometer but with snow charac-

teristics similar to the surface below the radiometers. Sea ice thickness was measured with an ice auger (5 cm in diameter) every 7 days by averaging the data obtained from three close sites. The measurement accuracy of ice thickness was ±0.5 cm.

As the snow thickness and other surface properties are measured manually at noon time, the albedo at 1200 LST was used in this study, and the zenith angle at local noon was lower than 80° from 25 August onward in both 2010 and 2011.

3. Evolution of the observed albedo, atmospheric condition and surface properties

Time series of the incoming and outgoing shortwave radiation, albedo, surface temperature, snow thickness, and ice thickness from 25 August to 15 December 2010 and from 25 August to 30 November 2011 are shown in Fig. 3. In response to the spring–summer transition, both shortwave and longwave radiation components increased steadily (figure not shown).
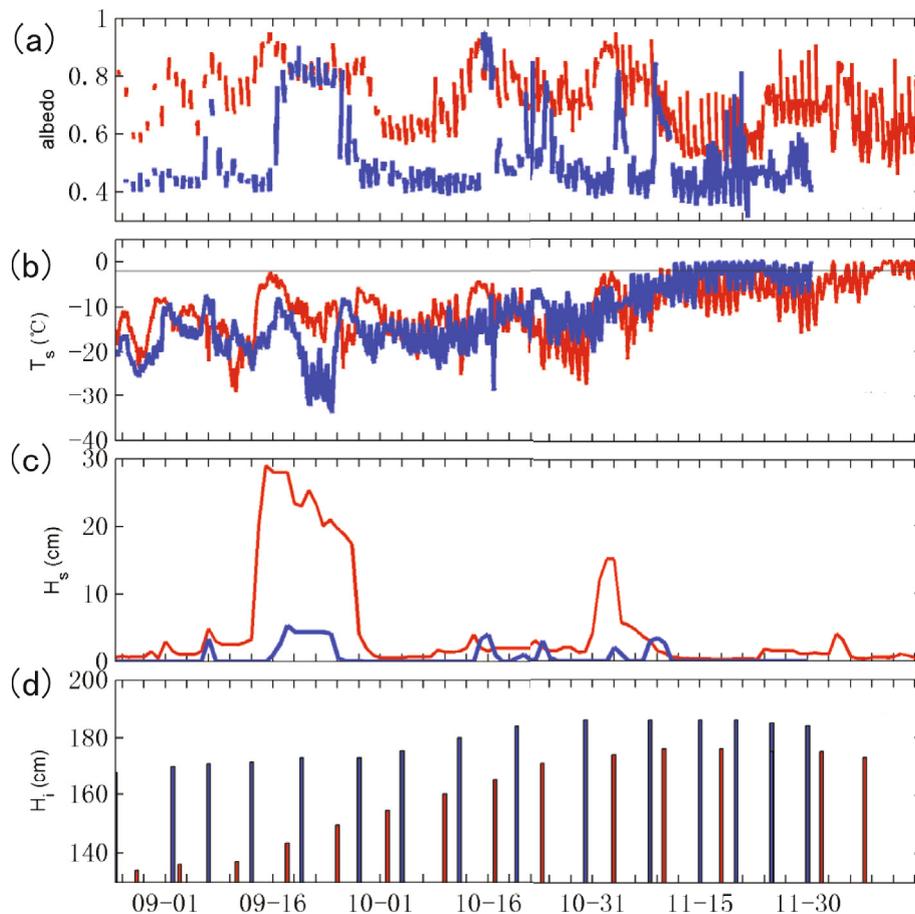
Fig. 3. Time series of (a) albedo for solar zenith angles less than 80°, (b) surface temperature, (c) daily snow thickness, and (d) daily ice thickness from 25 August to 15 December, 2010, and from 25 August to 30 November, 2011. The red and blue lines (dots) represent the results from 2010 and 2011, respectively.

3.1. Observed albedo in 2010

The daily averaged surface temperature varied from $-26.0°C$ to $-0.2°C$, and the daily maximum was slightly above $0°C$ after 3 December (Fig. 3b). The ice surface was covered (or partially covered) with snow during the entire observation period. The mean snow thickness during the observation period was 4.0 cm, but it was below 2.0 cm during most of the observation period. Snow thickness was larger than 10 cm during 15–27 September and 3 November, with the largest value of 29 cm on 15 September (Fig. 3c). Dominated by sea ice thermodynamics, the ice thickness increased from 133 ± 2 cm on 28 August to 176 ± 2 cm 10 November—rapidly between mid-September and the end of October. The ice thickness in November is close to the thermodynamic equilibrium between heat loss to the atmosphere and heat gain from ocean water, latent heat of freezing, solar heat flux and air–sea interaction. Finally, the ice thickness was 173 ± 2 cm on 8 December (Fig. 3d).

The mean albedo was 0.70 during the 2010 campaign. The surface was under metamorphism with the air temperature increasing, and the monthly mean albedo decreased from 0.80 in September to 0.62 in December. The highest albedos were at times the snow layer was thick, during snowfall and blowing-snow events. There were 26 days with a noon albedo higher than 0.8. Taking the period 13 September to 28 September as an example, an intermittent snowfall associated with snowstorms occurred. When the surface was covered with a thin layer of fresh dry snow (snow thickness of ~3.0 cm), the albedo was 0.83 on 13 September, and from 14–16 September, with the new snowfall, it was higher than 0.9. The albedo peaked at 0.94 on 15 September, when the new, fresh snow accumulation was 29 cm thick and with a grain size smaller than 1 mm. Because of the low surface air temperature and strong winds (Fig. 2a), a hard frozen layer formed at the surface on 18 September. As a result, the albedo decreased to 0.81 and remained at this level until 24 September, when a new 1-cm fresh snow layer increased the albedo to 0.86. The surface was covered with a hard frozen layer again on 25–28 September, and the albedo was within 0.76–0.83. A strong wind on 28–29 September blew away most of the snow cover, and the albedo decreased to 0.68.

There were 24 days with a noon albedo lower than 0.6; most of these measurements were associated with a thin, hard snow layer or melting snow surface (0–1 cm snow thickness). Specifically, there was no snowfall during 1–8 October, and the surface was covered with 0–1 cm of hard snow. The albedo under clear and overcast skies was 0.58–0.60 and 0.62–0.65, respectively. During 12–23 November, the surface was covered by a 0–1 cm thin wet snow layer with grains that were wet and soft and 1–3 mm in size, and then the albedo under clear and overcast skies was 0.51–0.54 and 0.56–0.63, respectively. On 6–13 December, the surface air temperature was usually above $0°C$ and the albedo varied between 0.49 and 0.59 (except for 9 December, when it was 0.69), which signified a surface of approximately 70% melting snow (1.0–1.2 cm) and 30% bare ice. Because the surface snow and ice were just under the melting temperature, there was a 0–1 cm surface wet snow layer. The albedo under clear and overcast skies during 6–13 December was 0.50–0.51 and 0.54–0.63, respectively, although a slight increase to 0.7 was noted on 9 December due to weak snowfall. The minimum albedo of 0.46 was observed in the afternoon of 12 December when it was under clear sky.

3.2. Observed albedo in 2011

Both snow thickness and surface albedo were much smaller than in 2010, which can be partly attributed to less snowfall and more clear skies in 2011 than in 2010 (Fig. 2). In 2011, the surface was bare ice during most of the observation period, and the mean snow thickness was 0.8 cm, with most of the observation period without snow cover, which led to a mean albedo of 0.49. Over the 99-day observation period, there were 55 days with an albedo below 0.45. And the minimum albedo was as low as 0.36 in mid-November, when the surface layer was melting. Our observations showed an albedo of 0.41 for bare ice under a clear sky, which is 0.08 lower than Brandt et al. (2005). Possible reasons contributing to the difference include the fact that our observations were based on the 1200 LST value when the solar zenith angle was near its daily minimum (the albedo was also near its daily minimum), while the observation time of Brandt et al. (2005) was random. A 0.15 inter-diurnal variation was shown in our observations, and Vihma et al. (2009) also observed a similar variation (0.14); the difference of 0.08 is among the range of inter-diurnal variation. Our values were based on direct measurements on the ice surface, while Brandt et al. (2005) used ship-born sensors. There was also a difference in the spectral bands. The measurements of Brandt et al. (2005) covered the wavelength regions of 320–1060 nm (Voyage 1988 and 1996) and 320–1800 nm (with a gap of 1000–1115 nm in Voyage 2000), while our measurement range was 310–2800 nm. Furthermore, they summarized the albedo from numerous types of sea-ice surface types in the Southern Ocean (Brandt et al., 2005), while our observation site was fixed in a local coastal landfast sea-ice zone near Zhongshan Station.

During the measurement period of 2011, the ice thickness increased from 167 ± 2 cm on 24 August to the maximum of 186 ± 2 cm on 30 October, and remained at this level until 20 November when melt slowly started. The daily average surface temperature increased from $-28.9°C$ to $-0.7°C$, while the instantaneous surface temperature in the afternoon reached the melting point on 14 November, 20 days earlier than that in 2010 (Fig. 3).

There were six snowfall or blowing-snow (blizzard) events, which led to a snow accumulation of more than 2 cm, resulting in a relatively high albedo (>0.6). The highest albedo (0.94) was observed during a snowfall event on 15 October. One month earlier, after a snowfall event that started on 16 September, the maximum dry snow thickness (5.3 cm) occurred on 18 September, corresponding to a high albedo of 0.83. The snow thickness was greater than 4 cm between 18 and 24 September, and the albedo was within 0.77–0.83.

The fresh snow brought by the other five falling/blowing-snow events (6–7 September, 14–15 October, 24 October, 3 November and 9 November) was blown away shortly after its accumulation, and each of the five relatively high albedo periods lasted only 1–2 days.

3.3. *Effects of synoptic events and clouds*

Clearly, snowfall, blowing snow and other synoptic events have a significant influence on the albedo by changing surface properties (Grenfell and Perovich, 1984), i.e., snowfall can increase the albedo by increasing snow thickness and bringing new surface snow particles.

We compared the albedo under snowfall with the albedo under a clear sky (or less cloudiness) on adjacent days during the 2010 observation period, and there were 14 pairs in total. This albedo increased from 0.13 to 0.29, and with an average of 0.18 among all the 14 pairwise comparisons. From August to December 2010, the total number of snowfall days at Zhongshan Station reached 67, which accounted for 44.7% of the total days and showed that frequent snowfall events have a major effect on the albedo. In contrast, our field observations suggest that, on the one hand, blowing snow (gales) may increase the surface snow thickness and reduce the surface grain size, but on the other hand, the wind may blow away all the accumulated snow at the surface. Consequently, topography and wind direction are also factors affecting albedo during blowing-snow events, and it is very difficult to add these effects into parameterization schemes.

Clouds can absorb infrared solar radiation, and snow/ice has strong absorption in the infrared band. Because of multiple reflections, the albedo under cloudy skies is higher than that under clear skies (Warren, 1982). Grenfell and Perovich (1984) showed that the albedo under a cloudy sky is 5%–10% higher than that under a clear sky. We compared the albedo of the same ice and snow surfaces on adjacent days of clear (or less cloudy) days with 100% cloudy days. The albedo under a cloudy sky was higher than that under a clear sky, and the difference ranged from 0.03 to 0.09 with an average of 0.06. Brandt et al. (2005) suggested that for the Antarctic sea ice, the dry snow and wet snow albedos were 0.07 and 0.06 higher under a cloudy sky than under a clear sky, respectively. Our observations are consistent with these results. The fraction of days during which there was full cloud cover reached 53.1% and 43.6% in the observation periods of 2010 and 2011, respectively; thus, the effects of clouds should also be considered in parameterization schemes.

4. Evaluation of albedo parameterizations in climate models

Following Liu et al. (2007), four existing snow/ice albedo parameterizations ranging from simple to complex were evaluated in this study. The parameterization of Parkinson and Washington (1979) only considers broadband albedo for snow and bare ice (PW79). The Alfred Wegener Institute Regional Climate Model for the Arctic Region (Dethloff et

al., 1996; HIRHAM) considers the dependence of albedo on surface temperature. The Arctic Regional Climate System Model (Lynch et al., 1995; ARCSYM) includes the impacts of snow thickness and ice thickness on the albedo. Besides weighting snow and sea ice albedos with snow thickness, the albedo scheme used in CCSM3 further distinguishes the visible and near-infrared albedos (Briegleb et al., 2004). For a detailed description of these parameterizations, see Parkinson and Washington (1979), Lynch et al. (1995), Dethloff et al. (1996), Briegleb et al. (2004) and Liu et al. (2007).

Figure 4 shows the observed and simulated albedos during the measurement period. The observed surface conditions from Zhongshan Station (surface temperature, air temperature, snow thickness, and ice thickness) were used to calculate the albedos. The PW79 parameterization overestimated the observed mean albedo, both in 2010 (+0.05) and in 2011 (+0.09), and failed to capture the observed albedo variations in 2010.

The HIRHAM parameterization underestimated the observed mean albedo in 2010 (−0.06) but overestimated the albedo in 2011 (+0.14). HIRHAM did not match the observed albedo when the surface temperature was below the melting point. In fact, it reached a minimum when the observations reached their maximum on 15 September 2010 (Fig. 4a). However, HIRHAM could reproduce the observed gradual variation in albedo, when the surface temperature approached the melting point (Figs. 4a and b). Because the surface temperature is the only dependent parameter, the HIRHAM scheme could not reproduce the observed increase in albedo during snowfall events. Additionally, as surface temperature is near the melting point during the summer period, the parameterized albedo tended to oscillate by approximately 0.30 (Figs. 4a and b). This underestimates albedo, especially when the surface is covered by a snow layer (e.g., in 2010).

By considering the surface temperature, snow thickness and ice thickness, the ARCSYM parameterization captured the observed seasonal transitions in albedo during both spring and summer melting periods (Figs. 4a and b). The ARCSYM scheme produced a good result in summer 2010 but greatly overestimated the albedo during the 2011 melting period, e.g., the ARCSYM albedo in 2011 was always higher than 0.5, whereas the observed albedo minimum was lower than 0.4. In addition, it could not reproduce the observed rapid drop-off associated with sea ice melt.

For the most complex case, the CCSM3 scheme showed the best result among the four parameterizations. The mean bias was −0.03 in 2010 and 0.08 in 2011. However, CCSM3 did not produce an albedo higher than 0.80 and highly overestimated the bare ice albedo in 2011. Also, it did not reproduce the observed rapid drop-off during the melting period.

The correlations between the observed albedo and the surface parameters (surface temperature, snow thickness or ice thickness) measured near Zhongshan Station were calculated to determine the most important factors affecting albedo. The correlation coefficients between albedo and snow thickness in 2010 and 2011 were 0.55 and 0.89, while the correlation co-
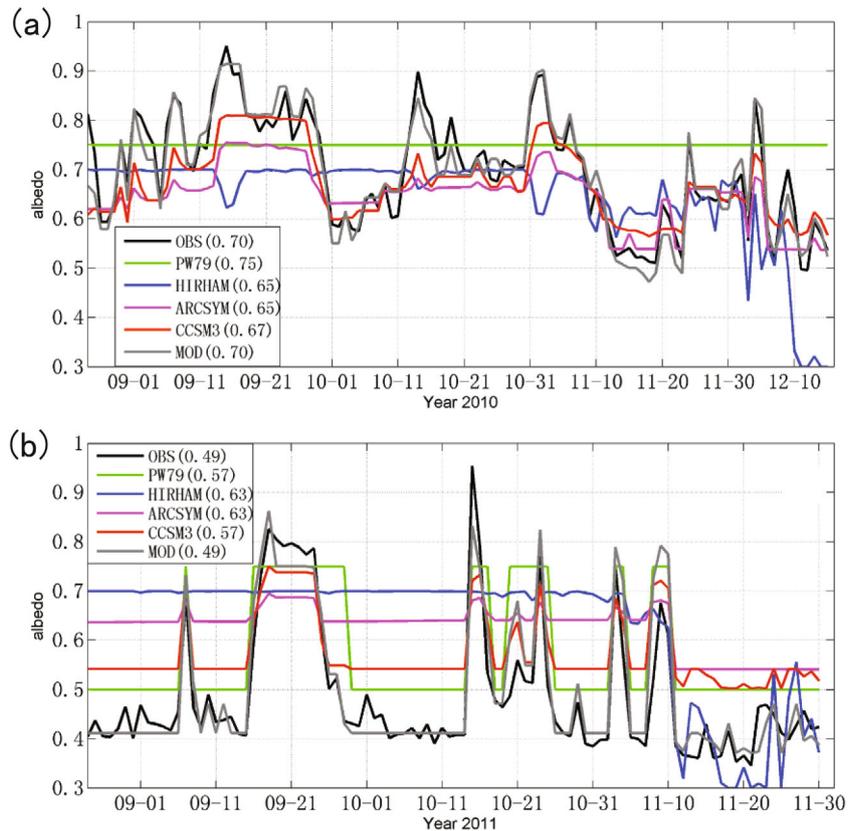
Fig. 4. Daily average observed surface albedo and parameterized surface albedos (a) from 25 August to 15 December, 2010 and (b) from 25 August to 30 November, 2011 (the averaged albedo for the four parameterizations over the entire period is shown in parentheses).

efficients between albedo and ice thickness were -0.43 and -0.16, respectively. This suggests that albedo and ice thickness are not correlated significantly when the ice is thicker than the optical thickness of ice. The result is consistent with former studies (Barry, 1996; Curry et al., 2001; Liu et al., 2007). The correlations between albedo and surface temperature in 2010 and 2011 were -0.27 and -0.30, respectively. However, this negative correlation between albedo and surface temperature was very weak before 1 November, when surface temperature was far below the melting point; the correlations in 2010 and in 2011 were 0.42 and -0.10, respectively. There was a strong negative correlation between albedo and surface temperature after 1 November, when surface temperature approached the melting point gradually; their correlation coefficients in 2010 and 2011 were -0.49 and -0.61, respectively. The albedo dependence on surface temperature is related to the fact surface properties change as surface temperature approaches 0°C (Liston et al., 1999; Pirazzini, 2004). After removing the effects of snow thickness, the partial correlations of the albedo and surface temperature were -0.28 and -0.25 in 2010 and 2011, respectively. In contrast, the partial correlations of the albedo and snow thickness were still high (0.56 and 0.89). This further indicates that snow thickness plays the more important role in determining albedo.

To develop a parameterization that is suitable for Antarctic landfast sea ice, we made three modifications to the CCSM3 parameterization (Table 1). In CCSM3, the bare-ice albedos in the visible and near-infrared bands were 0.73 and 0.33 (Table 1), respectively, while Brandt et al. (2005) reported characteristic values of 0.67 and 0.29 (<0.7 and >0.7 μm), respectively. As discussed in section 3.2, our observations show a characteristic value of 0.41 for bare ice under clear sky in 2011, which is 0.08 lower than the value of Brandt et al. (2005). Assuming that the difference in our data is independent of spectral band, subtracting 0.08 from these values suggests visual and near-infrared albedo values of 0.59 and 0.21 (Table 1, row 1). This modification is helpful for simulations of low albedo over bare ice or melting ice.

In addition, snowfall events can influence albedo remarkably. As discussed previously, snowfall and 100% cloud cover may result in an increase in albedo by 0.18 and 0.06, respectively. The CCSM3 parameterization can only reflect the effects of changes in snow-cover thickness. In addition to snow thickness, we assume that other effects can contribute a 50% increase (0.09), and a simple formula that describes the albedo increase caused by snowfall and cloud cover is proposed (Table 1, row 2). This adjustment is important for the simulation of a high albedo, especially during or just after a snowfall event. As the snowfall amount can be obtained from an atmospheric model, this simple scheme can also be used in other parameterizations.

Table 1. Differences between the modified snow/ice albedo parameterization and CCSM3

Dependence	CCSM3	Modified parameterization
Bare-ice albedo	$\left\{\begin{array}{l} \alpha_{i-\text{vis}} = 0.73 \\ \alpha_{i-\text{nir}} = 0.33 \end{array}\right\}$	$\left\{\begin{array}{l} \alpha_{i-\text{vis}} = 0.59 \\ \alpha_{i-\text{nir}} = 0.21 \end{array}\right\}$
Albedo increase due to snowfall and clouds	Not considered	$\left\{\begin{array}{l} \alpha_{\text{sc}} = 0.09 \text{(with snowfall)} \\ \alpha_{\text{sc}} = 0.06 \text{(when cloud cover is 100\% and there is no snowfall)} \\ \alpha_{\text{sc}} = 0 \text{(for other cases)} \end{array}\right\}$
Fraction of surface snow cover	$H_{\text{s}}/(H_{\text{s}} + 0.02)$	$H_{\text{s}}/(H_{\text{s}} + 0.01)$

Notes: α, albedo; H_{s} snow thickness; vis, visible band (<0.7 μm); nir, near-infrared band (>0.7 μm); i, ice; sc, snow cover.

In CCSM3, the fraction of surface snow cover is expressed as $H_{\text{s}}/(H_{\text{s}} + 0.02)$, where H_{s} is snow thickness in units of m, and the value of 0.02 was selected to reach good agreement with SHEBA data (Briegleb et al., 2004). To better reflect the influence of snow thickness, expressions should be modified to fit for the local horizontal surface of the Antarctic landfast sea ice. According to the local feature that the snow thickness during the campaign was thinner than SHEBA, and the fact that the 0.01-m thick snow cover can have a large impact on the albedo, we modified the expression to $H_{\text{s}}/(H_{\text{s}} + 0.01)$ (Table 1, row 3).

As shown in Fig. 4, the modified parameterization shows much better agreement with observed albedos in 2010 and 2011. The mean $\pm$ standard deviation biases of the parameterized albedo were -0.00 ± 0.03 and 0.01 ± 0.05 in 2010 and 2011 (Table 2), respectively, relative to the observations. Furthermore, the parameterized albedo can effectively capture both the high and low albedo limits and the observed rapid drop-off in the melting period.

5. Conclusions

To understand the variations of Antarctic sea ice albedo and factors influencing its variations, and to evaluate the performance of current albedo parameterizations over Antarctic sea ice, we continuously measured the in-situ albedo over Antarctic coastal landfast sea ice in Prydz Bay, near Zhongshan Station. The observation periods covered austral spring and early summer of 2010 and 2011, which can be considered as representative of albedo evolution over Antarctic coastal landfast sea ice during the seasonal transition. The mean observed albedos in 2010 and 2011 were 0.70 and 0.49, respectively. The large difference of 0.21 was attributed to less snow accumulation in 2011. Synoptic events and cloud cover have a significant influence on albedo, leading to an average increase of 0.18 and 0.06 associated with snowfall and overcast skies, respectively.

Using the observations, we examined the performance of different existing snow/sea ice albedo algorithms succeed in simulating variations in sea-ice albedo over the Antarctic coastal landfast sea ice. The four selected albedo schemes showed significantly different albedo evolutions from spring to early summer and, in general, the complex schemes considering snow thickness and the spectral distribution of

Table 2. Mean and standard deviation (STD) biases of parameterized surface albedos relative to the observations.

Albedo scheme	Mean bias		STD bias	
	2010	2011	2010	2011
PW79	0.05	0.08	0.11	0.08
HIRHAM	-0.05	0.14	0.11	0.15
ARCSYM	-0.05	0.14	0.07	0.11
CCSM3	-0.03	0.09	0.06	0.07
MOD	-0.00	0.01	0.03	0.05

incoming radiation produced a more reasonable albedo than the simple ones, particularly during the summer melting period. This is consistent with a previous study over Arctic sea ice (Liu et al., 2007). Both correlation and partial correlations showed that snow thickness is the most important factor in determining the albedo and should be added in albedo schemes. Considering two spectral bands, the CCSM3 parameterization showed the best result among all the parameterizations. However, it could not reflect an observed albedo higher than 0.80, nor capture the observed rapid drop-off during the melting period, and highly overestimated the bare ice and melting albedo in 2011.

Based on the observational analysis in this study, a modified parameterization was developed based on the CCSM3 parameterization. By further considering the effects of synoptic events and cloud cover, as well as the local landfast sea-ice surface characteristics, the modified parameterization effectively captured the observed variations in the albedo. As the snowfall information can be obtained from weather or climate models, this parameterization can be easily applied. However, it should be noted that further evaluations with more field observations over Antarctic sea ice are still strongly recommended.

REFERENCES

Allison, I., R. E. Brandt, and S. G. Warren, 1993: East Antarctic sea ice: Albedo, thickness distribution, and snow cover. *J. Geophys. Res.*, **98**(C7), 12 417–12 429.

Barry, R. G., 1996: The parameterization of surface albedo for sea ice and its snow cover. *Progress in Physical Geography*, **20**(1), 63–79.

Brandt, R. E., S. G. Warren, A. P. Worby, and T. C. Grenfell, 2005: Surface albedo of the Antarctic sea ice zone. *J. Climate*, **18**(17), 3606–3622.

Briegleb, B. P., C. M. Bitz, E. C. Hunke, W. H. Lipscomb, M. M. Holland, J. L. Schramm, and R. E. Moritz, 2004: Scientific description of the sea ice component in the community climate system model, version 3. NCAR/TN-463+STR.

Curry, J. A., J. L. Schramm, D. K. Perovich, and J. O. Pinto, 2001: Applications of SHEBA/FIRE data to evaluation of snow/ice albedo parameterizations. *J. Geophys. Res.: Atmos.*, **106**(D14), 15 345–15 355.

Dethloff, K., A. Rinke, R. Lehmann, J. H. Christensen, M. Botzet, and B. Machenhauer, 1996: Regional climate model of the Arctic atmosphere. *J. Geophys. Res.*, **101**(D18), 23 401–23 422.

Fraser, A. D., R. A. Massom, K. J. Michael, B. K. Galton-Fenzi, and J. L. Lieser, 2012: East Antarctic landfast sea ice distribution and variability, 2000–08. *J. Climate*, **25**(4), 1137–1156.

Grenfell, T. C., and D. K. Perovich, 1984: Spectral albedos of sea ice and incident solar irradiance in the southern Beaufort Sea. *J. Geophys. Res.: Oceans*, **89**(C3), 3573–3580.

Heil, P., S. Gerland, and M. A. Granskog, 2011: An Antarctic monitoring initiative for fast ice and comparison with the Arctic. *The Cryosphere Discussions*, **5**(5), 2437–2463.

Hoppmann, M., M. Nicolaus, P. A. Hunkeler, P. Heil, L.-K. Behrens, G. König-Langlo, and R. Gerdes, 2015: Seasonal evolution of an ice-shelf influenced fast-ice regime, derived from an autonomous thermistor chain, *J. Geophys. Res.: Oceans*, **120**, 1703–1724, doi: 10.1002/2014JC010327.

Järvinen, O., and M. Leppäranta, 2013: Solar radiation transfer in the surface snow layer in Dronning Maud Land, Antarctica. *Polar Science*, **7**, 1–17.

Lei, R. B., Z. J. Li, B. Cheng, Z. H. Zhang, and P. Heil, 2010: Annual cycle of landfast sea ice in Prydz Bay, east Antarctica. *J. Geophys. Res.: Oceans*, **115**(C2), doi: 10.1029/2008JC005223.

Leppäranta, M., O. Järvinen, and E. Lindgren, 2013: Mass and heat balance of snow patches in Basen nunatak, Dronning Maud Land in summer. *J. Glaciol.*, **59**(218), 1093–1105.

Liston, G. E., O. Bruland, H. Elvehoy, and K. Sand, 1999: Below-surface ice melt on the coastal Antarctic ice sheet. *J. Glaciol.*, **45**(150), 273–285.

Liu, J. P., and J. A. Curry, 2010: Accelerated warming of the Southern Ocean and its impacts on the hydrological cycle and sea ice. *Proceedings of the National Academy of Sciences of the United States of America*, **107**(34), 14 987–14 992.

Liu, J. P., Z. Zhang, J. Inoue, and R. M. Horton, 2007: Evaluation of snow/ice albedo parameterizations and their impacts on sea ice simulations. *Int. J. Climatol.*, **27**(1), 81–91.

Lynch, A. H., W. L. Chapman, J. E. Walsh, and G. Weller, 1995: Development of a regional climate model of the western Arctic. *J. Climate*, **8**(6), 1555–1570.

Parkinson, C. L., and W. M. Washington, 1979: A large-scale numerical model of sea ice. *J. Geophys. Res.: Oceans*, **84**(C1), 311–337.

Parkinson, C. L., and D. J. Cavalieri, 2012: Antarctic sea ice variability and trends, 1979–2010. *The Cryosphere*, **6**(2), 871–880.

Perovich, D. K., and C. Polashenski, 2012: Albedo evolution of seasonal Arctic sea ice. *Geophys. Res. Lett.*, **39**(8), doi: 10.1029/2012GL051432.

Perovich, D. K., T. C. Grenfell, B. Light, and P. V. Hobbs, 2002: Seasonal evolution of the albedo of multiyear Arctic sea ice. *J. Geophys. Res.*, **107**(C10), SHE 201-1–SHE 20-13.

Pirazzini, R., 2004: Surface albedo measurements over Antarctic sites in summer. *J. Geophys. Res.: Atmos.*, **109**(D20), doi: 10.1029/2004JD004617.

Pirazzini, R., T. Vihma, M. A. Granskog, and B. Cheng, 2006: Surface albedo measurements over sea ice in the Baltic Sea during the spring snowmelt period. *Ann. Glaciol.*, **44**, 7–14.

Smith, I. J., P. J. Langhorne, T. G. Haskell, H. Joe Trodahl, R. Frew, and M. R. Vennell, 2001: Platelet ice and the land-fast sea ice of McMurdo Sound, Antarctica. *Ann. Glaciol.*, **33**, 21–27.

Vihma, T., M. M. Johansson, and J. Launiainen, 2009: Radiative and turbulent surface heat fluxes over sea ice in the western Weddell Sea in early summer. *J. Geophys. Res.: Oceans*, **114**(C4), doi: 10.1029/2008JC004995.

Warren, S. G., 1982: Optical properties of snow. *Rev. Geophys.*, **20**(1), 67–89.

Weiss, A. I., J. C. King, T. A. Lachlan-Cope, and R. S. Ladkin, 2012: Albedo of the ice covered Weddell and Bellingshausen Seas. *The Cryosphere*, **6**, 479–491.

Wendler, G., B. Moore, D. Dissing, and J. Kelley, 2000: On the radiation characteristics of Antarctic sea ice. *Atmos.-Ocean*, **38**(2), 349–366.